Supplementary Information

Supplementary Figures

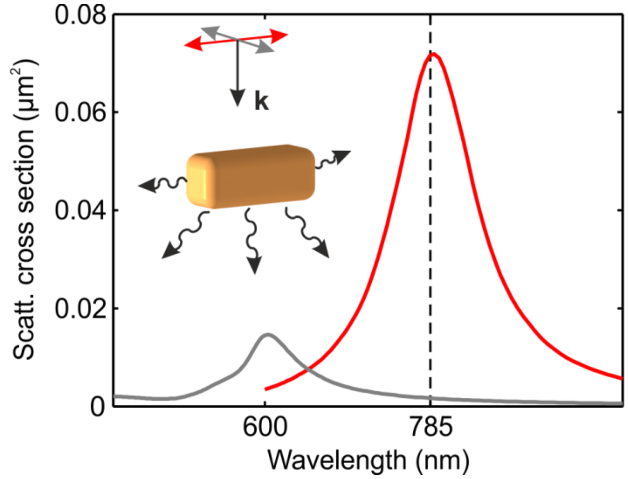

Supplementary Figure 1| Scattering cross section of a gold nanorod. Numerically calculated scattering cross sections of a gold nanorod are shown for incident light polarized along the long-axis (*x*-polarization, red curve) and short axis (*y*-polarization, gray curve). At $\lambda = 785$ nm, *x*-polarized incident light is resonantly scattered. This effect is much weaker for *y*-polarized incident light.

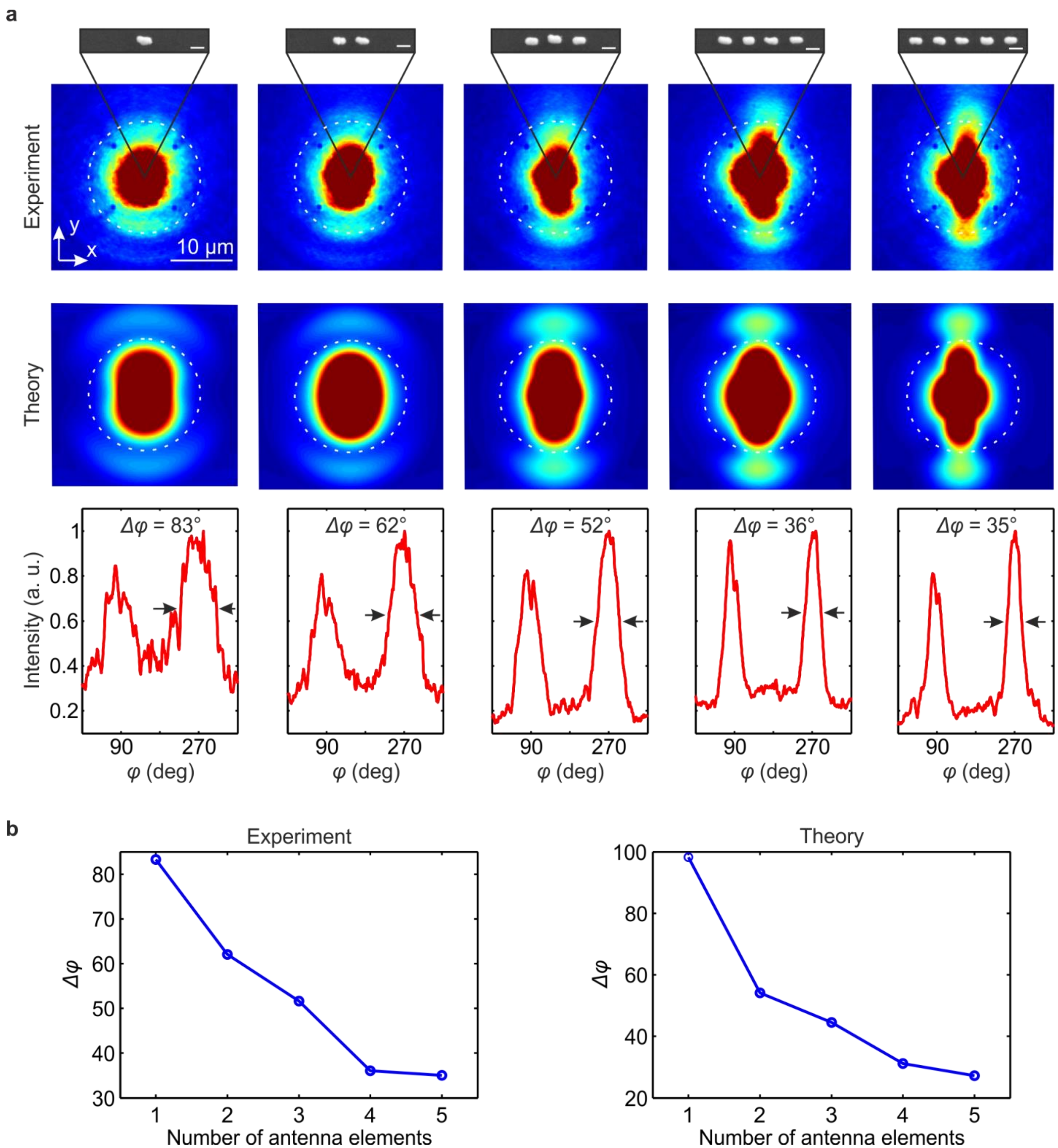

Supplementary Figure 2 | Antenna arrays increase the directivity of the radiation pattern. a, The luminescence pattern around the antenna array becomes significantly narrower as the number of antenna elements is increased (top row, 100 nm scale bars in the scanning electron micrographs). The experimental results are in good agreement with theory (second row, see details about model in Methods). The narrowing of the radiation pattern is seen even more clearly in the plot of the fluorescence intensity along the white dashed circles (bottom row). **b,** The narrowing of the radiation pattern saturates at five antenna elements due to the finite width of the incident beam driving the nanoantenna array. In this case the array radiates a directive beam and the size of the array (850×50 nm^2) is still much smaller than a square wavelength.

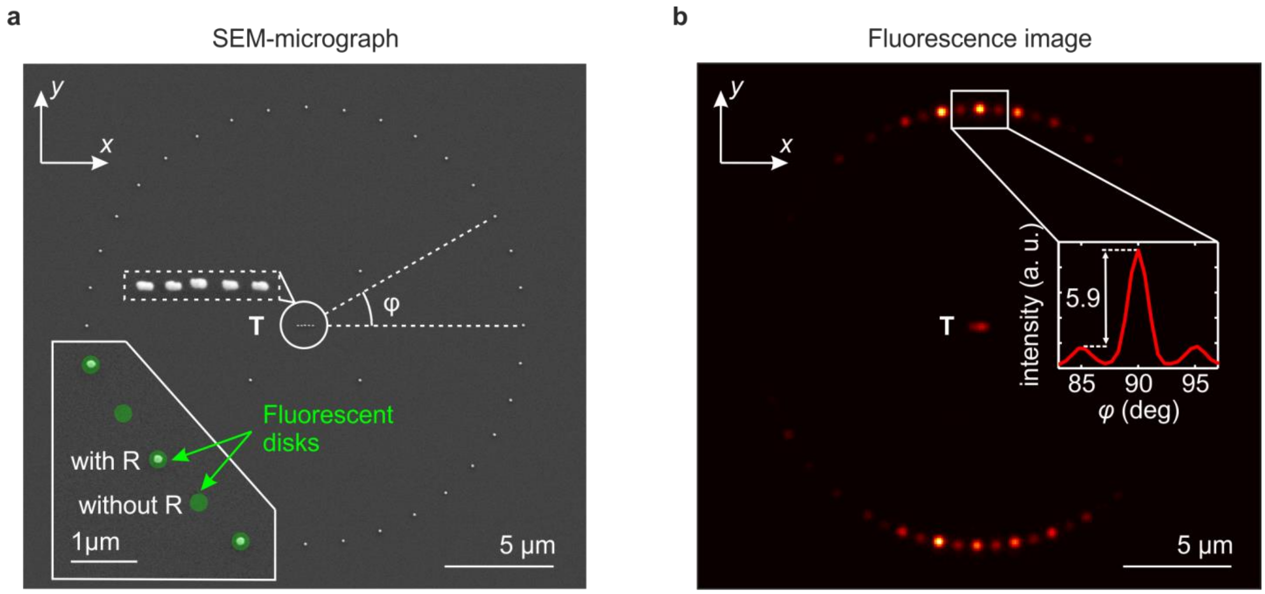

Supplementary Figure 3 | Plasmonic wireless antenna link with receivers around nanoantenna array transmitter. a, Scanning electron micrograph of the device. Gold nanodisk receivers R are positioned on a circle (radius 10 µm) around nanoantenna array transmitter T. Receiving fluorescent disks are positioned on top and in between plasmonic antennas (inset). **b,** Fluorescence image when the transmitter is excited with *x*-polarized incident light without phase gradient across the antenna array. Receivers in the ±*y*-direction light up and an intensity enhancement of 6 is observed for every second receiver due to the additional receiving plasmonic antenna. Plasmonic antennas at a distance of 3.5 µm to the antenna along the y-direction receive only 25% of radiation. Therefore the cross talk is rather low and the spacing between the receiving antennas could be reduced further. More directional antennas such as Yagi-Uda structures would improve the directionality and reduce the crosstalk.

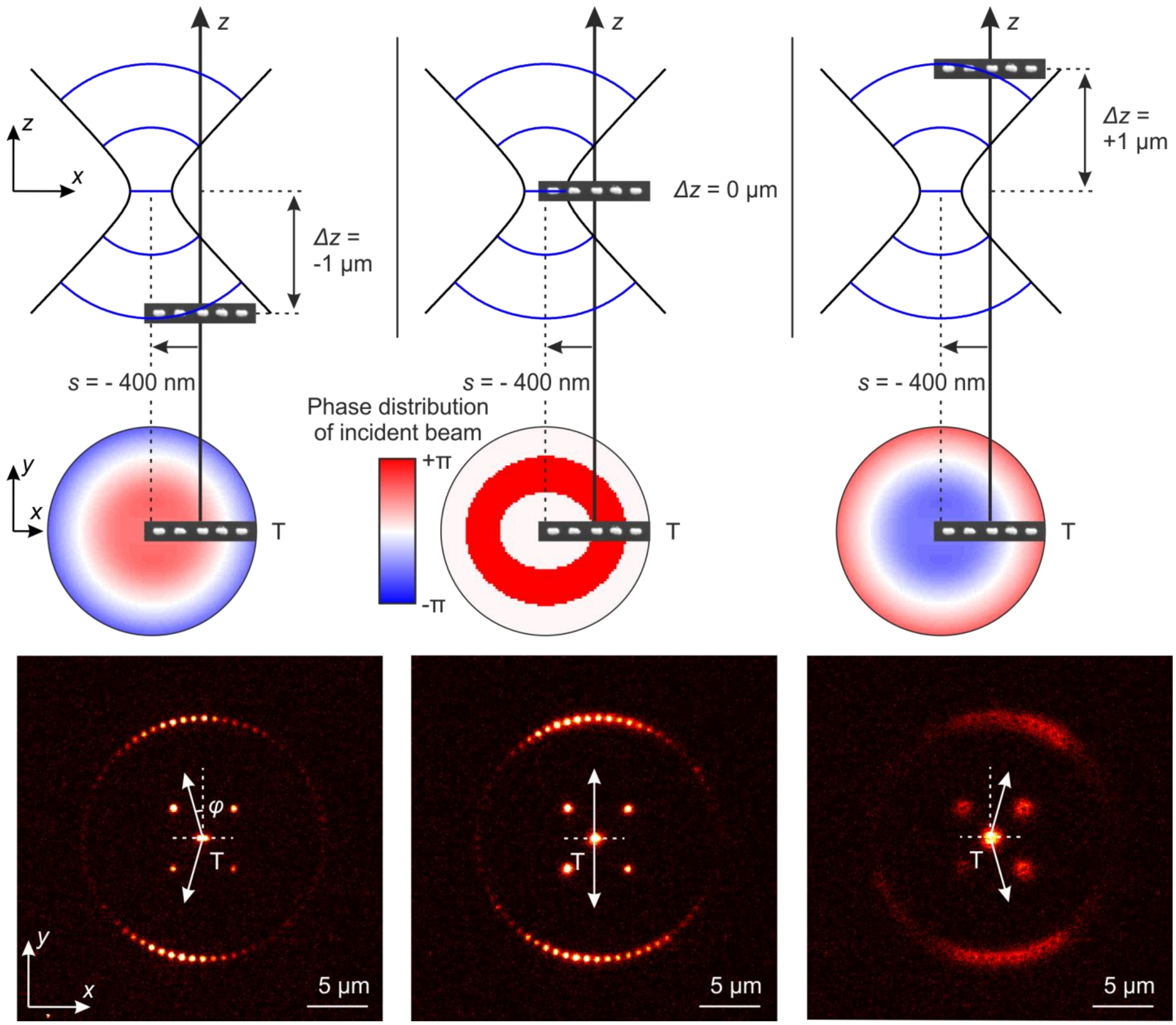

Supplementary Figure 4 | Influence of shift through focus on the beamsteering direction. We study the radiation pattern around a single five element antenna array at different focus positions when the incident beam is positioned at the left end of the antenna array (*s* = -400 nm, top row). The radius of curvature of the incident wave fronts reverses sign when we move the sample through the focus along the *z*-direction. Hence the phase gradient across the antenna array reverses sign when we perform a *z*-scan. The phasing of the antenna array and hence the transmitted beam direction is similar to the phasing when we shift the incident beam laterally from the left to the right end of the antenna array for a fixed *z*-plane (Δz = -1 µm, see Fig. 4 and Supplementary Fig. 5). This leads to a rerouting of the transmitted radiation from left to right and vice versa observed in the luminescent images of the bottom row. The radiation pattern is mapped by luminescent disk receivers around the transmitter in a similar manner as in Fig. 4. We observe a reversal of the steering direction as we pass through the focus due to the change of the curvature of the wavefronts of the incident field. The change in quality of the luminescence images for different *z*-values is due to aberrations of our objective (bottom row).

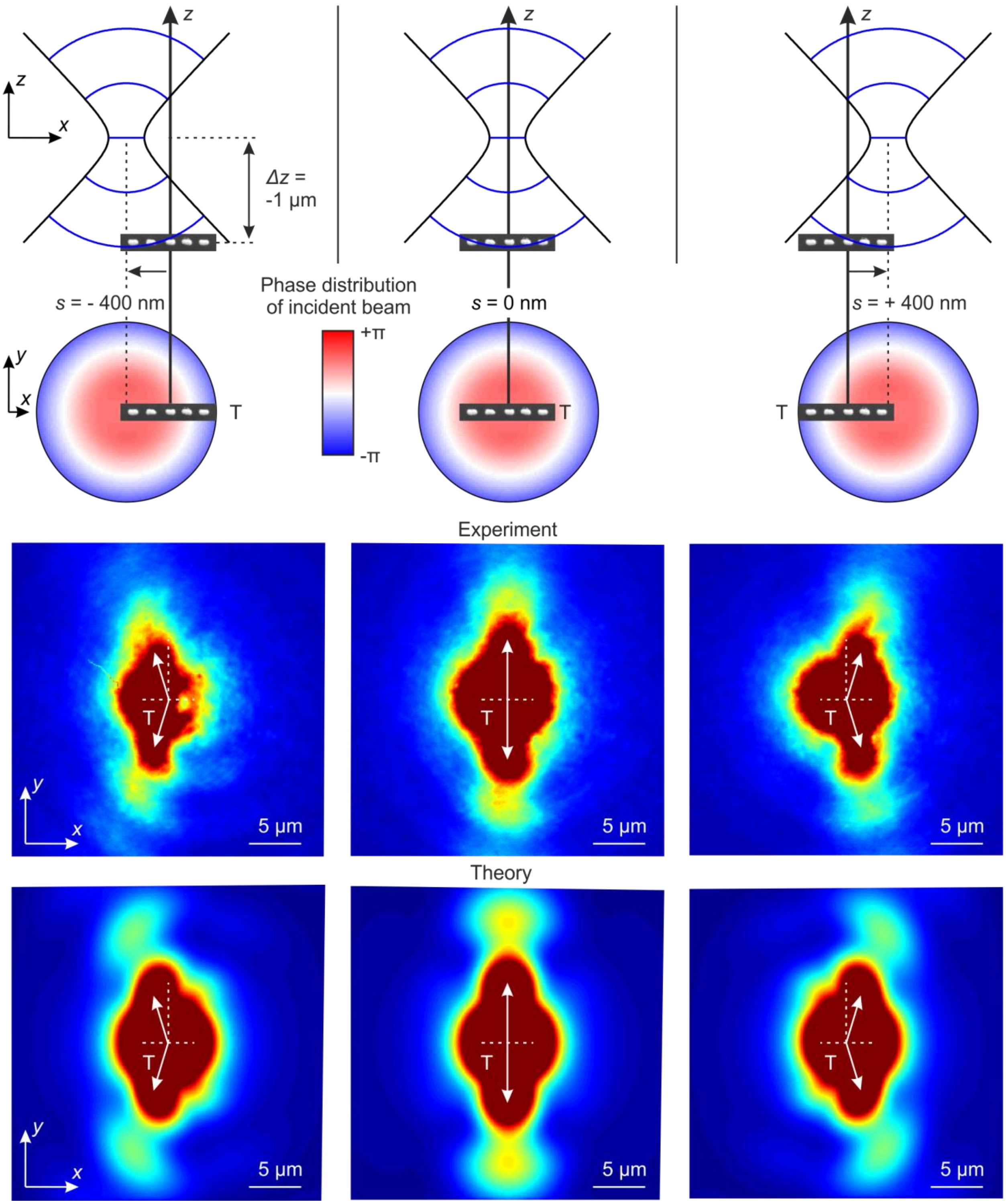

Supplementary Figure 5 | Beamsteering using nanoantenna arrays. We displace the incident spot laterally by 400 nm from the nanoantenna array, inducing a phase gradient across the structure (top row; the scanning electron micrographs of the antenna array T are to scale with the calculated wavefronts and phase distributions). We observe controllable beamsteering upon shifting the incident beam laterally (middle row). The experimental data of the resulting emission pattern are in very good agreement with theory (bottom row).